Propylene Polymerization with α-Keto-β-Diimine Initiators Proceeds via Enantiomorphic Site Control

ARTICLE *in* MACROMOLECULES · MAY 2012

Impact Factor: 5.8 · DOI: 10.1021/ma300504j

8 AUTHORS, INCLUDING:

Gerald Kehr
University of Münster
363 PUBLICATIONS **8,018** CITATIONS
SEE PROFILE

Fumihiko Shimizu
Mitsubishi Chemical Group Science and Techn…
22 PUBLICATIONS **370** CITATIONS
SEE PROFILE

Griselda Barrera Galland
Universidade Federal do Rio Grande do Sul
97 PUBLICATIONS **1,647** CITATIONS
SEE PROFILE

Macromolecules

Article

pubs.acs.org/Macromolecules

Propylene Polymerization with α-Keto-β-Diimine Initiators Proceeds via Enantiomorphic Site Control

Jason D. Azoulay,[†] Haiyang Gao,[‡] Zachary A. Koretz,[†] Gerald Kehr,[§] Gerhard Erker,[§] Fumihiko Shimizu,[⊥] Griselda B. Galland,*[,∥] and Guillermo C. Bazan*[,†]

[†]Departments of Chemistry & Biochemistry and Materials, Center for Polymers and Organic Solids, University of California Santa Barbara, Santa Barbara, California, United States

[‡]Institute of Polymer Science, School of Chemistry and Chemical Engineering, Sun Yat-Sen University, Guangzhou, China

[§]Organisch-Chemisches Institut der Universität Münster, Corrensstrasse 40, 48149 Münster, Germany

[⊥]Corporate Strategy Division, Mitsubishi Chemical Chemical Corporation, 14-1, Shiba 4-chome, Minato-ku, Tokyo 108-0014, Japan

[∥]Instituto de Química, Universidade Federal do Rio Grande do Sul, Av. Bento Gonçalves, 9500-CEP: 91501-970 Porto Alegre, Brazil

Supporting Information

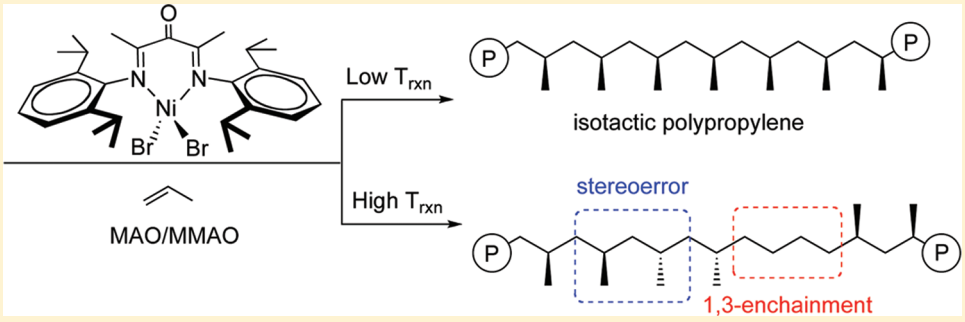

ABSTRACT: ^{13}C NMR spectroscopy is used to characterize the microstructure of polypropylene (PP) obtained using a nickel α-keto-β-diimine initiator activated with methylaluminoxane (MAO) at different reaction temperatures (T_{rxn}). The product prepared at −20 °C has structural features that resemble an ethylene-propylene copolymer. We find that the main sequences present in this sample arise as a result of normal 1,2-insertion and that propylene sequences are predominantly isotactic (m = 88%, $mmmm$ = 63%). There is also evidence of ethylene-like sequences as a result of 3,1-enchainment, and from 2,1-insertion. A reduction in T_{rxn} to −60 °C results in a polymer that has undetectable regioirregularities and is highly isotactic (m = 93%, $mmmm$ = 85%). Moreover, the application of stereo propagation models gives indication that the isospecificity is a result of enantiomorphic site control.

INTRODUCTION

Polyolefins constitute a wide range of commodity products with enormous economic impact.[1−4] The variety of materials that can be generated from simple monomer feedstocks emanates, in part, from the development and design of transition metal systems capable of facile insertion into the metal carbon bond and through tailoring of the coordination environment of the metal center. In this context, a long-standing goal in polyolefin synthesis lies in generating stereoregular poly(1-alkenes), such as polypropylene (PP). Stereochemical control has been achieved by using heterogeneous (Ziegler−Natta) and homogeneous olefin polymerization catalysts.[1−9] In homogeneous systems, the stereoselectivity of monomer insertion can be dictated by the coordination environment at the metal center afforded by ancillary ligands (enantiomorphic site control) or via the growing polymer chain (chain-end control).[5] A spectrum of PP materials exhibiting a wide range of physical properties can thereby be obtained. It is therefore of interest to gain access to novel PP structures and to understand how new olefin polymerization catalysts and initiators can be used to mediate stereocontrol.

While there are many examples of stereoselective propylene polymerization catalysts, there are few examples that are living.[2−9] Stereoselective late transition metal systems remain relatively rare due to the propensity to generate amorphous polymers as a result of poor regioselectivity and chain-end isomerization processes.[10−14] A noteworthy example includes C_2-symmetric α-diimine Ni(II) complexes, which produce highly isotactic polypropylene (*i*PP) through enantiomorphic-site control at low temperatures.[15] The *i*PP generated using these complexes is structurally different to those obtained using metallocene based systems as a result of microstructures generated via chain-walking events.[16,17] Furthermore, the distinctive features of late transition metal systems in combination with living behavior have allowed

Received: March 13, 2012
Revised: May 1, 2012
Published: May 17, 2012

Scheme 1. Complex 1 and the Resulting Propylene Polymerization

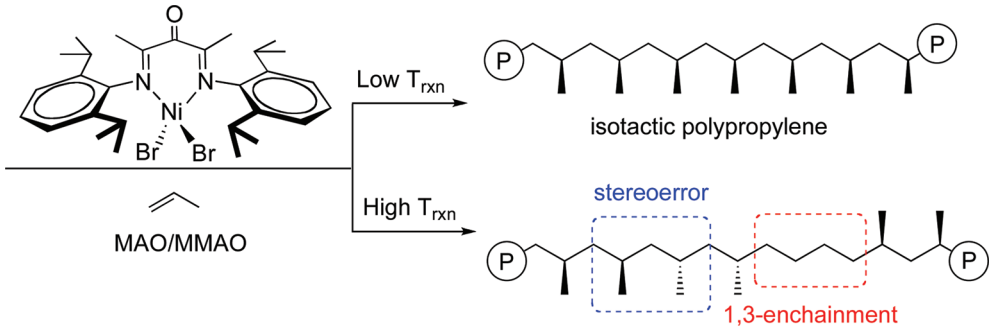

Table 1. Propylene Polymerization Data for 1/MAO or MMAO[a]

entry	propylene (mL)	activator	T_{rxn} (°C)	time (h)	yield (mg)	TOF[b] (h^{-1})	M_n[c] (g/mol)	PDI[c]	T_m[d] (°C)	$[CH_3]/[CH_2]$[e]	% 1,3-[f]	[mmmm][g]	P_m[h]
1	10	MAO	25	1	950	2260	126 000	2.00	ND[i]	0.50	25	29	0.73
2	10	MAO	0	2	720	857	101 000	1.33	ND[i]	0.57	20	36	0.77
3	10	MAO	−10	2	580	690	79 000	1.05	59	0.64	16	43	0.81
4	20	MAO	−20	3	430	170	42 000	1.10	76	0.69	13	63	0.87
5	40	MAO	−40	6	95	19	7500	1.19	96	0.76	9	62	0.89
6	40	MAO	−40	6	150	30	11 900	1.26	97	0.76	9	63	0.89
7	40	MMAO	−40	6	175	35	11 600	1.28	95	0.75	10	60	0.88
8	40	MAO	−60	8	55	8	3400	1.32	132	1.00	0	86	0.96
9	40	MMAO	−60	8	90	13	6400	1.30	134	1.00	0	85	0.97

[a]Polymerization conditions: 10 μmol of **1** (entries 1−3) or 20 μmol of **1** (entries 4−9), 50 mL toluene (entries 1−5, 7−8) or 50 mL chlorobenzene (entries 6,9), [Al]/[Ni] = 250. [b]TOF (turnover frequency):mol propylene/(mol Ni·h). [c]Determined by gel permeation chromatography (GPC) in 1,2,4-trichlorobenzene (TCB) at 150 °C versus polystyrene standards. [d]Determined by DSC. [e]Determined by ^{1}H NMR spectroscopy. [f]1,3-enchainment, calculated from the equation: % 1,3-enchainment = $[(1 - R)/(1 + 2R)] \times 100$, where $R = [CH_3]/[CH_2]$. [g]Determined by quantitative ^{13}C NMR spectroscopy. [h]Probability of successive stereoregular insertion, calculated from the equation: $P_m = ([mmmm])^{1/4}$. [i]Not detected.

for the generation of novel materials such as ethylene-propylene (EP) type copolymers[18] and regio-block copolymers.[15] Bis(imino)pyridine iron complexes can also produce *i*PP through a 2,1-insertion mechanism that likely plays a role in stereoregulation.[19,20] Because of the increased tolerance of late transition metals toward functionalized alkenes controlling the stereoselectivity of the PP remains a noteworthy limitation for accessing novel polyolefin materials.[21−28]

A new type of late transition metal initiator was reported, which is supported by the α-keto-β-diimine ligand, i.e., complex **1** in Scheme 1. Active sites are generated by using coactivators such as methylaluminoxane (MAO). The presence of the carbonyl functionality on the ligand framework leads to a 2-order of magnitude increase in the rate of PE production, when compared to the activity observed with a related six-membered β-diimine analogue.[29,30] Furthermore, the **1**/MAO combination has been used to produce semicrystalline polyethylene, PP, and poly(1-hexene) under living polymerization conditions.[31]

It is also worth pointing out that the carbonyl group in the α-keto-β-diimine ligand not only has the potential to serve as a conduit for modification of electron density at the metal, but can also participate in deactivation reactions that must be carefully mitigated to achieve optimal control over the product properties. A discrete cationic nickel analogue of **1** showed increased polymerization rates upon binding of a Lewis acid to the exocyclic carbonyl functionality. It was also found that reaction with aluminum-alkyls commonly present in MAO solutions (i.e., $AlMe_3$) results in Al−C addition across the carbonyl functionality, rearrangement of the ligand framework and to a substantial decrease in the rate of polymerization.[32−37] Furthermore, the excess of aluminum (Al/Ni = 250 equiv) required to activate **1** complicates *in situ* observation and characterization of initiating/propagating sites.

In this work ^{13}C NMR spectroscopy is used to characterize the structural features of the products obtained from propylene polymerizations by using **1**/MAO at different reaction temperatures. The product prepared at −20 °C has structural features that are similar to those of an ethylene-propylene copolymer. We find that the main sequences present in this sample arise as a result of normal 1,2-insertion of propylene and that propylene sequences are predominantly isotactic (m = 88%, $mmmm$ = 62.7%). There are also a significant amount of ethylene-like sequences present as a result of 3,1-enchainment (11%) and from 2,1-insertion (4.4%) of the monomer. A reduction in T_{rxn} to −60 °C results in a polymer with undetectable regioirregularities and is found to be highly isotactic (m = 93%, $mmmm$ = 85%), a remarkable feature given the absence of an obvious chiral ligand environment in **1**.

RESULTS AND DISCUSSION

The **1**/MAO combination was evaluated in a series of propylene polymerizations designed to examine how the products change as a function of the reaction conditions (Table 1). These reactions involved condensing a specified amount of propylene into a 300 mL reactor loaded with 50 mL of toluene or chlorobenzene and MAO or MMAO so that [Al]/[Ni] = 250. We note here that volatiles were removed from commercially available MAO or MMAO solutions prior to use.[38] The reaction was subsequently equilibrated at the appropriate reaction temperature (T_{rxn}) and the polymerization was initiated by the introduction of 10 μmol of **1**.

dx.doi.org/10.1021/ma300504j | Macromolecules 2012, 45, 4487−4493

Comparison of entries 1 and 3 in Table 1 demonstrates that reducing T_{rxn} from 25 °C to −10 °C leads to a narrowing of the polydispersity (PDI) from 2.00 to 1.05, and a drop in the turnover frequency (TOF) and the number-average molecular weight (M_n) of the product. Changing the coactivator from MAO to a modified MAO (MMAO) leads to slightly elevated activities (TOF = 19 versus 35 h^{-1} respectively at −40 °C). Reactions carried out in chlorobenzene (entries 6 and 9) show higher propylene consumption than those performed in toluene and a corresponding increase in M_n. Reactions carried out below −20 °C exhibit elevated PDIs probably due to precipitation of the more crystalline polymer product. Differential scanning calorimetry (DSC) indicates that the polymer obtained at 25 °C is amorphous, while at −60 °C one observes a melting temperature (T_m) of 134 °C (entry 9). Intermediate T_m values are obtained between the lowest and highest reaction temperatures. Through this process of optimization, we determined that the highest activity at −60 °C was found using MMAO in chlorobenzene (entry 9 in Table 1).

NMR spectroscopy was used to provide insight into the polymer microstructure.[39,40] The ratio (0.50) of CH_3 to CH_2 integrals from ^{1}H NMR spectroscopy indicates that the product obtained at 25 °C is regioirregular, with (−CH_2−) sequences of various lengths in the polymer backbone.[15] From Table 1, one observes a nearly perfect PP structure ([CH_3]/[CH_2] ∼ 1) when the polymerization is carried out at −60 °C. Also at this temperature, no unsaturated chain ends were detected, indicating that minimal β-H elimination takes place during the time scale of polymer propagation or upon quenching with methanol (Supporting Information). This feature supports the hypothesis that the active centers are stable to chain termination at lower T_{rxn} with an increase in the PDI resulting from precipitation of the polymer product.

The microstructure of the polymerization product changes significantly with decreasing T_{rxn}. The ^{13}C NMR spectrum of the product obtained at −20 °C is shown in Figure 1.

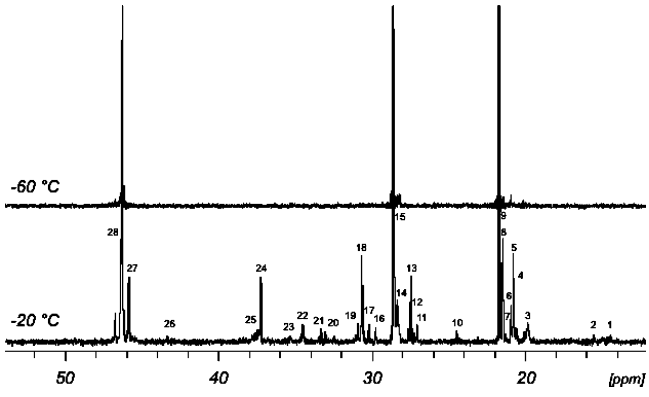

Figure 1. ^{13}C NMR spectra (125 MHz, 115 °C, 1,1,2,2-$C_2D_2Cl_4$) of the products obtained at −20 and −60 °C.

The spectra from products obtained at various T_{rxn} are shown in the Supporting Information. The corresponding experimental and calculated chemical shifts,[41] related sequences and assignments are shown in Table 2. The fourth column includes the triad sequences using the copolymer nomenclature adopted by refs 39 and 40. In this nomenclature, an ethylene unit is designated by the letter E, a propyl unit with P, which corresponds to a methyl branch and the inverted unit is marked by an asterisk. For the assignments P designates a primary carbon, S a secondary carbon, and T a tertiary carbon followed by Greek subscripts indicating the position relative to the nearest tertiary carbons in both directions along the polymer chain.[42] For clarity, letters for the carbon atoms and the numbers corresponding to the structure are shown in Figure 2. All the samples beside the one obtained at −60 °C resemble EP copolymers. At −20 °C the main structural feature present in all ^{13}C NMR spectra is the normal (1,2)-propylene insertion represented by PPP sequences at 19.5−22.0 ppm, which correspond to methyl carbons (*mmmm* at 21.82 ppm and *mmmr* at 21.59 ppm). The main methine and methylene resonances are present at 28.2−28.9 ppm and 46.3−46.9 ppm, respectively. Other resonances in these regions can be attributed to regioirregularities. Structures 1, 2, 3, 5, and 8 in Figure 2 arise as a result of a 3,1-enchaiment process. Regioerrors of this type likely occur via a 2,1-insertion of propylene, followed by subsequent chain-walking to the α-Me group to give a methylene $(-CH_2-)_3$ linkage in the polymer backbone (see Scheme 2).[10,16,17,39,40] Structures 4, 6, and 7 arise as a result of inversion of a propylene unit without chain walking.[43] While these are minor errors when T_{rxn} is very low, the percentage of 3,1-insertions increases at higher T_{rxn}. Addition of structures 1, 2, 3, 5, and 8 illustrates that at −20 °C there are approximately 13% of 3,1 insertions, which decreases to 9% at −40 °C.

Table 1 shows that with a decrease in T_{rxn}, the *mmmm* pentad (where *m* corresponds to adjacent methyl groups in a meso orientation) increases from 29% at 25 °C, to 86% at −60 °C. These structural features correspond to probabilities of successive stereoregular insertions (P_m) of 0.73 and 0.96, respectively.[43] Figure 1 also shows a ^{13}C NMR spectrum of the product obtained at −60 °C (entry 9 in Table 1). One observes sharp signals corresponding to isotactic PP (i.e., a predominant *mmmm* peak) with no evidence of 3,1-insertions. The polymer structure is therefore both regioregular and highly isotactic under these conditions.

Integration of the methine region can be used to quantify normal propylene sequences (PPP = I_{15}). The methyl region (resonances 3 to 9) is normally used to calculate the tacticity of the PP. However, due to the presence of regioerrors, the typical stereoerror calculation by using pentad distributions (i.e., *mmmr* or *mmrr*) is not as straightforward. In this sense, peak 3b not only represents the pentad PPPPP *mrrr* but also the triad EPE derived from alternating 3,1-enchainments (structure 2) and the sequence EP*PE + EP*PE from structure 8. Resonance 4 is the addition of contributions of PPPPP *mrmr* and the methyl carbon from structure 6. Resonance 5 can be attributed to EPP + PPE triads derived from sequences arising from 3,1 enchainment and from the contribution of the PPPPP *mmrm* + *rmrr* pentads. The only sample that has no regioirregularities is the one made at −60 °C. From these data, it is possible to calculate the mechanism of stereopropagation using the Bernoulli statistic (enantiomorphic site control) and the Markov statistic (chain end control) models.[44,45] Application of these equations using the observed stereo dyad (*m*) are listed in Table 3 where σ is the probability of generating a meso sequence when a new monomer unit is inserted at the end of a growing chain in the chain end control model, and the persistence probabilities for D configuration at a D preferring site and L configuration at an L preferring site in the enantiomorphic site control model.[44,46] The calculated triads and pentad (*mmmm*) for the enantiomorphic site model are in better agreement to the experimental sequences than the chain end model.

dx.doi.org/10.1021/ma300504j | *Macromolecules* 2012, 45, 4487−4493

Table 2. ^{13}C NMR Analysis of Isotactic Regioirregular PP: Experimental and Calculated Chemical Shifts, Sequences, and Assignments

	chemical shift			assignments		
peak	expt (ppm)	calcd (ppm)	sequence			
1	14.57	16.64	PP*P	$P_{\alpha\gamma}$	W	7
2	15.72	17.13	PP*P*+PPP*(head-to-head)	$P_{\alpha\beta}$	O	4
3	19.80−20.10	20.61	PPP(rr)		CH_3	
3a	19.82	20.61	PPPPP(mrrm)		CH_3	
3b	19.92	19.63	EPE	$P_{\delta\delta}$	F	2
		19.63	EPP*E+EP*PE	$P_{\gamma\delta}$	ρ	8
	19.98	19.61	PPPPP(mrrr)		CH_3	
3c	20.08−20.30	19.61	PPPPP(rrrr)		CH_3	
4	20.69	20.61	PPPPP(mrmr)		CH_3	
			P*P*PP+ P*P*PP (tail-to-tail)	$P_{\beta\gamma}$	V	6
5	20.86	20.61	PPPPP(mmrm+rmrr)		CH_3	
		20.12	EPP+PPE	$P_{\beta\delta}$	E	1
6	21.02	20.61	PPPPP (mmrr)		CH_3	
7	21.15−21.50	20.61	PPPPP(rmmr)		CH_3	
8	21.59	20.61	PPPPP(mmmr)		CH_3	
9	21.82	20.61	PPPPP(mmmm)		CH_3	
10	24.58	24.58	PEP	$S_{\beta\beta}$	S	5
11	27.16	27.27	EEPP+PPEE	$S_{\beta\delta}$	L	3
12	27.32	27.52	PPEE (r)	$S_{\beta\gamma}$	A	1
13	27.54	27.52	PPEE (m)	$S_{\beta\gamma}$	A	1
14	27.73	27.52	PEE+EEPE	$S_{\beta\gamma}$	I	2
15	28.2−28.9	28.38	PPP		CH	
	28.72		PPPPP(mmmm)		CH	
16	29.87	29.96	EEE	$S_{\delta\delta}$	N	3
17	30.29	30.21	EEEP+PEEE	$S_{\gamma\delta}$	M	3
18	30.77	30.45	EPP+PPE+	$T_{\beta\delta}$	C_vJ,	1, 3
19	31.01	30.45	P*P*PP+ P*P*PP (tail-to-tail)	$T_{\beta\delta}$	U	6
		31.53	PP*P	$S_{\beta\alpha\beta\delta}$	Y	7
20	33.13	32.52	EPE	$T_{\delta\delta}$	G	2
21	33.38	32.52	EPP*E+EP*PE	$T_{\gamma\delta}$	ω	8
22	34.60	34.47	P*P*PP+ P*P*PP (tail-to-tail)	$S_{\gamma\alpha\beta\delta}$	T	6
		34.22	EPP*E+EP*PE	$S_{\delta\alpha\beta\delta}$	ε	8
		34.72	P*PP	$S_{\gamma\alpha\beta\gamma}$	Z	7
23	35.49	34.99	PP*P*+PPP*(head-to-head)	$T_{\alpha\beta}$	P	4
24	37.34	37.16	PPEE+EEPP	$S_{\alpha\delta}$	B, K	1, 3
25	37.54−37.93	36.91	EPE+PEE	$S_{\alpha\delta}$	H	2
		37.41	PEP	$S_{\alpha\gamma}$	R	5
		37.06	PP*P	$T_{\alpha\gamma}$	X	7
26	43.26	41.42	PP*P*+PPP*(head-to-head)	$S_{\beta\alpha\alpha\gamma}$	Q	4
27	45.95	44.11	PPE+EPPP	$S_{\alpha\alpha}$	D	1
28	46.37	44.36	PPPPP(m)	$S_{\alpha\alpha}$	CH_2	
	46.84	44.36	PPP(rr)	$S_{\alpha\alpha}$	CH_2	

Quantitative equations for all the regio and stereo sequences are listed in Table 4 where I_x represents the integrals used to calculate each sequence. As those materials resemble EP copolymers, the sequences are presented as if they were from an EP copolymer. In Table 5 the structures listed in Figure 2 and named from 1 to 8 are related to a specific carbon atom representative of each structure or a combination of them. In the last column the integrals used to calculate the amount of each structure are also listed.

Table 6 lists the results of the application of the above quantitative analyses to the samples obtained at −20 °C (entry 4) and −60 °C (entry 9) for which respective spectra are shown in Figure 1. The sample obtained at −60 °C is highly isotactic (m = 93%, $mmmm$ = 85%) and follows an enantiomorphic site mechanism. The sample obtained at −20 °C is an isotatic polypropylene (m = 88%, $mmmm$ = 63%) with regioirregularities (P* = 4.4%) and with a considerable amount of methylene sequences as a result of 3,1-enchainment (E = 11%).

CONCLUSION

In conclusion, we report that the polymerization of propylene by using the **1**/MAO combination can generate a range of products with microstructures ranging from highly isotactic and regioregular PP at low temperatures to atactic and regioirregular polymers at high temperatures. ^{13}C NMR characterization of the isotactic PP microstructure provides evidence that stereoselectivity in the propagation sequence arises as a result

dx.doi.org/10.1021/ma300504j | Macromolecules 2012, 45, 4487−4493

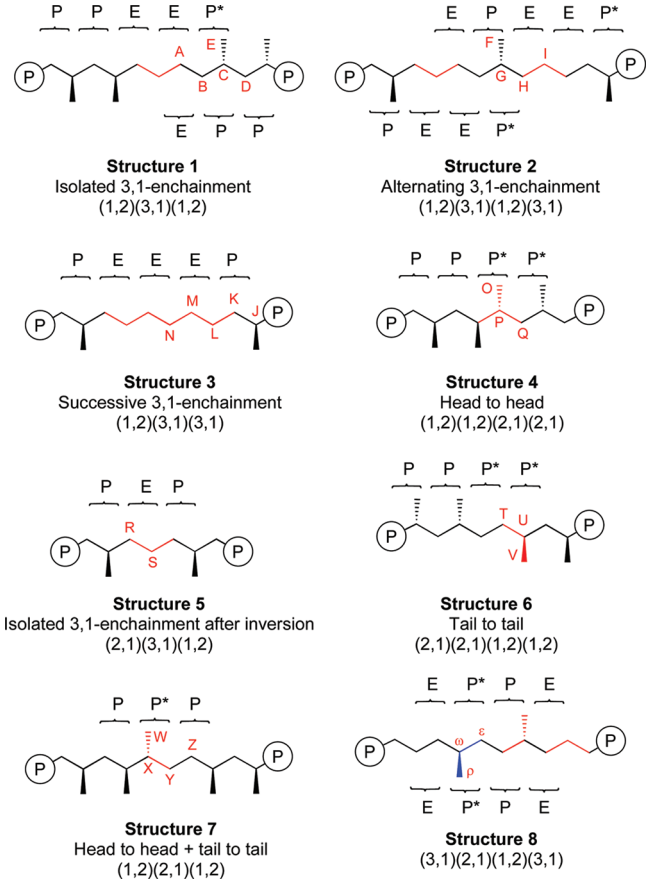

Figure 2. Structures in regioirregular products.

of enantiomorphic site control. It is interesting to note that the initiator precursor, namely compound **1**, lacks a chiral environment. These results are in contrast to other late metal systems that generally yield amorphous and atactic PP in the absence of chiral ligands[47,48] or that induce syndiotactic enchainment at lower temperatures.[49] We note, however, that the presence of the carbonyl functionality at the α-site of the ligand structure opens the possibility of binding Lewis acidic species in the MAO or MMAO solutions. Such an event has the potential to considerably change the coordination environment at nickel.

Table 3. Application of Stereo Propagation Models: Calculated and Observed Sequences

	m	σ	*mm*	*mr*	*rr*	*mmmm*
enantiomorphic site model		0.964	0.895	0.070	0.035	0.831
chain end model		0.930	0.865	0.130	0.005	0.748
experimental	0.93		0.895	0.069	0.035	0.850

Table 4. Quantitative Equations for Isotactic PP: Sequences and Tacticity

sequence	calculation from integrals
[PPP]	I_{15}
[EPP + PPE]	I_{18}
[EPE]	I_{20}
[EEE]	$I_{16}/2$
[EEP + PEE]	$I_{11} + I_{12} + I_{13} + I_{14}$
[PEP]	I_{10}
[PP*P* + PPP*]	$(I_{23} + I_{26})/2$
[P*PP + P*P*PP]	$I_{19} - I_1$
[PP*P]	I_1
[EP*PE + EP*PE]	I_{21}
mmmm	I_9
mmmr	I_8
rmmr	I_7
mmrr	I_6
mmrm + rmrr	$I_5 - I_{18}$
mrmr	$I_4 - (I_{19} - I_1)$
rrrr	I_{3c}
mrrr	$I_{3b} - I_{21} - I_{20}$
mrrm	I_{3a}

EXPERIMENTAL SECTION

General Remarks. All manipulations of air and/or water sensitive compounds were performed under an inert atmosphere using standard glovebox and Schlenk-line techniques. Dichloromethane (CH_2Cl_2) was distilled from CaH_2. Toluene was purchased from Aldrich (anhydrous grade) and used as received. MAO (methylaluminoxane solution, 10 wt % in toluene) was purchased from Aldrich and MMAO-3A (7 wt % Al in heptane) was purchased from Akzo-Nobel and dried *in vacuo*, until a free-flowing white powder was obtained. Propylene (99.97%) was purchased from Matheson Trigas and purified by passing through Agilent moisture and oxygen traps. Complex **1** was synthesized as previously reported.[29] NMR spectra

Scheme 2. Formation of *iso*-PP and 3,1-Regioerrors

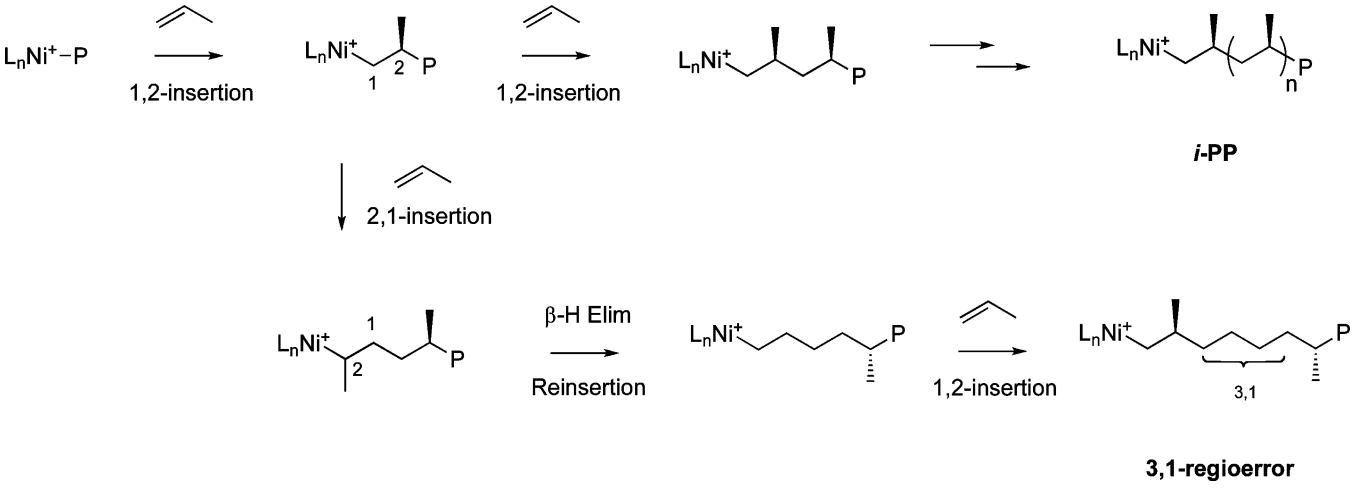

dx.doi.org/10.1021/ma300504j | *Macromolecules* 2012, 45, 4487–4493

Table 5. Quantitative Analysis for Structures Listed in Figure 2

structure	carbon atom	calculation from integrals
	CH	I_{15}
1	A	$I_{12} + I_{13}$
2	G	I_{20}
3	(L + M)/2	$(I_{11} + I_{17})/2$
4	(P + Q)/2	$(I_{23} + I_{26})/2$
5	S	I_{10}
6	U	$I_{19}-I_1$
7	W	I_1
8	ω	I_{21}

Table 6. Percentage of Sequences of Samples Obtained at Different Temperatures

	% at reaction temperature	
sequence	−20 °C	−60 °C
[PPP]	70.90	100.00
[EPP + PPE]	12.86	0.00
[EPE]	0.72	0.00
[EEE]	0.49	0.00
[EEP + PEE]	9.15	0.00
[PEP]	1.50	0.00
[P*P* + PP*P*]	1.25	0.00
[P*P*PP] + P*P*PP	1.31	0.00
[PP*P*P]	0.85	0.00
[EP*PE + EP*PE]	0.98	0.00
[P]	84.5	100.00
[E]	11.1	0.00
[P*]	4.4	0.00
mmmm	62.7	85.0
mmmr	19.8	3.6
rmmr	2.5	0.9
mmrr	5.0	3.4
mmrm + rmrr	0.0	2.1
mrmr	1.8	1.4
rrrr	2.3	1.3
mrrr	3.2	1.2
mrrm	2.8	1.0
mm	84.9	89.5
mr + rm	6.8	6.9
rr	8.3	3.5
m	88.3	93.0
r	11.7	7.0
0	82.9	100.0
1	7.9	0.0
2	0.8	0.0
3	1.5	0.0
4	1.5	0.0
5	1.7	0.0
6	1.5	0.0
7	1.0	0.0
8	1.1	0.0

were obtained using Bruker 500 MHz spectrometers and were referenced using signals from the 1,1,2,2-tetrachloroethane-d_2 solvent at 115 °C. TOFs were calculated from the mass of the product obtained. Polymers were characterized by GPC analysis, relative to polystyrene standards, at 135 °C in 1,2,4-trichlorobenzene (high-temperature chromatograph, PL-GPC 220). Polymer melting points (T_m) were measured on a TA Instruments differential scanning calorimeter (model DSC Q20) at a rate of 10 °C/min for three cycles using a temperature range of −30 to +180 °C

Polymerization of Propylene. A 300 mL Parr steel autoclave reactor, equipped with an addition funnel, was loaded inside a glovebox with toluene or chlorobenzene (50 mL) and solid MAO or MMAO so that [Al]/[Ni] = 250. A specified amount of nickel complex **1** in dichloromethane was added to the addition funnel from a freshly made stock solution. The reactor was sealed inside the glovebox. The reactor was then cooled in a dry ice/acetone bath and a specified volume of propylene was transferred into the reactor. The reactor was brought to the appropriate T_{rxn} and the polymerization was initiated via injection of the solution of **1** under argon. The T_{rxn} was controlled by means of a dry ice/acetone bath and found to be ±2 °C as monitored by an internal thermocouple. The reaction at a desired time was quenched by loading the addition funnel with methanol (10 mL) and injecting the methanol, under argon, directly into the stirring reaction mixture. The polymer was precipitated with methanol, collected by filtration, and washed with acidified methanol (10% HCl), methanol, and acetone sequentially and dried under high vacuum to a constant weight.

■ ASSOCIATED CONTENT

Ⓢ Supporting Information

Details of the synthesis and characterization of the polymers. This material is available free of charge via the Internet at http://pubs.acs.org.

■ AUTHOR INFORMATION

Corresponding Author

*Fax: 1-805-893-5270. Telephone: 1-805-893-5538. E-mail: bazan@chem.ucsb.edu, griselda.barrera@ufrgs.br.

Notes

The authors declare no competing financial interest.

■ ACKNOWLEDGMENTS

J.D.A. and G.C.B. are grateful for financial support from the Mitsubishi Chemical Center for Advanced Materials and the Department of Energy. G.B.G. is grateful to CNPq (Conselho Nacional de Desenvolvimento Científico e Tecnológico), Brazil. G.E. and G.K. gratefully acknowledge support from the Deutsche Forschungsgemeinschaft. G.C.B. is also a Bessel Awardee of the Humboldt Foundation.

■ REFERENCES

(1) Kaminsky, W. *Macromol. Chem. Phys.* **2008**, *209*, 459.
(2) Rieger, B.; Baugh, L.; Striegler, S.; Kacker, S. *Late Transition Metal Polymerization Catalysis*; John Wiley & Sons: New York, 2003.
(3) Blom, R.; Follestad, A.; Rytter, E.; Tilset, M.; Ystenes, M. *Organometallic Catalysts and Olefin Polymerization: Catalysts for a New Millennium*; Springer-Verlag: Berlin, 2001.
(4) Hoff, R.; Mathers, R. T. *Handbook of Transition Metal Polymerization Catalysts*: John Wiley & Sons: New York, 2010.
(5) Coates, G. W. *Chem. Rev.* **2000**, *100*, 1223.
(6) Resconi, L.; Cavallo, A.; Fait, A.; Piemontesi, F. *Chem. Rev.* **2000**, *100*, 1253.
(7) Makio, H.; Terao, H.; Iwashita, A.; Fujita, T. *Chem. Rev.* **2011**, *111*, 2363.
(8) Alt, H. G.; Köppl, A. *Chem. Rev.* **2000**, *100*, 1205.
(9) Hlatky, G. G. *Chem. Rev.* **2000**, *100*, 1347.
(10) Johnsohn, L. K.; Killian, C. M.; Brookhart, M. *J. Am. Chem. Soc.* **1995**, *117*, 6414.
(11) Ittel, S. D.; Johnson, L. K.; Brookhart, M. *Chem. Rev.* **2000**, *100*, 1169.
(12) Guan, Z.; Cotts, P. M.; McCord, E. F.; McLain, S. J. *Science* **1999**, *283*, 2059.
(13) Leatherman, M. D.; Svedja, S. A.; Johnson, L. K.; Brookhart, M. *J. Am. Chem. Soc.* **2003**, *125*, 3068.

(14) Meinhard, D.; Wegner, M.; Kipiani, G.; Hearley, A.; Reuter, P.; Fischer, S.; Marti, O.; Rieger, B. *J. Am. Chem. Soc.* **2007**, *129*, 9182.
(15) Cherian, A. E.; Rose, J. M.; Lobkovsky, E. B.; Coates, G. W. *J. Am. Chem. Soc.* **2005**, *127*, 13770.
(16) Orta, C. R.; Blazquez, J. F.; Wile, A. M. A.; Coates, G. W.; Alamo, R. G. *Macromolecules* **2011**, *44*, 3436.
(17) McCord, E. F.; McLain, S. J.; Nelson, L. T. J.; Arthur, S. D.; Coughlin, E. B.; Ittel, S. D.; Johnson, L. K.; Tempel, D.; Killian, C. M.; Brookhart, M. *Macromolecules* **2001**, *34*, 362.
(18) Rose, J. M.; Deplace, F.; Lynd, N. A.; Wang, Z.; Hotta, A.; Lobkovsky, E. B.; Kramer, E. J.; Coates, G. W. *Macromolecules* **2008**, *41*, 9548.
(19) Small, B. L.; Brookhart, M. *Macromolecules* **1999**, *32*, 2120.
(20) Babik, S. T.; Fink, J. *J. Mol. Catal. A. Chem.* **2002**, *188*, 245.
(21) McLain, S. J.; Sweetman, K. J.; Johnsohn, L. K.; McCord, E. F. *Polym. Mater. Sci. Eng.* **2002**, *86*, 320.
(22) Propeny, C. S.; Camacho, D. H.; Guan, Z. *J. Am. Chem. Soc.* **2007**, *129*, 10062.
(23) Diamanti, S. J.; Ghosh, P.; Shimizu, F.; Bazan, G. C. *Macromolecules* **2003**, *36*, 9731.
(24) Held, A.; Bauers, F. M.; Mecking, S.; Friedrich, S. K. *Chem. Commun.* **2000**, 301.
(25) Bauers, F. M.; Mecking, S. *Macromolecules* **2001**, *34*, 1165.
(26) Korthals, B.; Schnetmann, I. G.; Mecking, S. *Organometallics* **2007**, *26*, 1311.
(27) Nakamura, A.; Ito, S.; Nozaki, K. *Chem. Rev.* **2009**, *109*, 5215.
(28) Boardman, B. M.; Bazan, G. C. *Acc. Chem. Res.* **2009**, *42*, 1597.
(29) Azoulay, J. D.; Rojas, R. S.; Serrano, A. V.; Ohtaki, H.; Galland, G. B.; Bazan, G. C. *Angew. Chem., Int. Ed. Engl.* **2009**, *48*, 1089.
(30) Feldman, J.; McClain, S. J.; Parthasarathy, A.; Marshall, W. J.; Calabrese, J. C.; Arthur, S. D. *Organometallics* **1997**, *16*, 1514.
(31) Azoulay, J. D.; Schneider, Y.; Galland, G. B.; Bazan, G. C. *Chem. Commun.* **2009**, 6177.
(32) Azoulay, J. D.; Koretz, Z. A.; Wu, G.; Bazan, G. C. *Angew. Chem., Int. Ed. Engl.* **2010**, *49*, 7890.
(33) Chen, E. Y-X.; Marks, T. J. *Chem. Rev.* **2000**, *100*, 1391.
(34) Tian, J.; Hustad, D.; Coates, G. W. *J. Am. Chem. Soc.* **2001**, *123*, 5134.
(35) Mitani, M.; Furuyama, R.; Mohri, J.; Saito, J.; Ishii, S.; Terao, H.; Kashiwa, N.; Fujita, T. *J. Am. Chem. Soc.* **2002**, *124*, 7888.
(36) Hasan, T.; Ioku, A.; Nishii, K.; Shiono, T.; Ikeda, T. *Macromolecules* **2001**, *34*, 3142.
(37) Busico, V.; Cipullo, R.; Cutillo, F.; Friederichs, N.; Ronca, S.; Wang, B. *J. Am. Chem. Soc.* **2003**, *125*, 12402.
(38) Volatiles were removed from a commercially available MAO solution (10 wt %, Aldrich), until a free flowing white powder was obtained. MMAO is a modified methylaluminoxane activator containing 25% isobutyl aluminoxane prepared by the controlled hydrolysis of trimethylaluminum and triisobutylaluminum.
(39) Galland, G. B.; Da Silva, L. P.; Dias, M. L.; Crosetti, G. L.; Ziglio, C. M.; Filgueiras, C. A. L. *J. Polym. Sci: Part A: Polym. Chem.* **2004**, *42*, 2171.
(40) Dias, M. L.; Da Silva, L. P.; Crossetti, G. L.; Galland, G. B.; Filgueiras, C. A. L.; Ziglio, C. M. *J. Polym. Sci: Part A: Polym. Chem.* **2006**, *44*, 458.
(41) Linderman, L. P.; Adams, J. Q. *Anal. Chem.* **1973**, *43*, 1245−1252.
(42) Carman, C. J.; Harrington, P. A.; Wilkes, C. E. *Macromolecules* **1977**, *10*, 536.
(43) Hagihara, H.; Shiono, T.; Ikeda, T. *Macromol. Chem. Phys.* **1998**, *199*, 2439.
(44) Shelden, R. A.; Fueno, T.; Tsunetsugu, T.; Furukawa, J. *J. Polym. Sci., Polym. Lett.* **1965**, *3*, 23.
(45) Bovey, F. A.; Tiers, G. V. D. *J. Polym. Sci.* **1960**, *44*, 173.
(46) Odian, G. *Principles of Polymerization*, 4th ed.; John Wiley & Sons: New York, 2004; p 711.
(47) Killian, C. M.; Tempel, D. J.; Johnson, L. K.; Brookhart, M. *J. Am. Chem. Soc.* **1996**, *118*, 11664.
(48) For partially isotactic PP ([*mm*] = 0.41) using an α-diimine Ni(II) system, see: Pappalardo, D.; Mazzeo, M.; Antinucci, S.; Pellechia, C. *Macromolecules* **2000**, *33*, 9483.
(49) Pellechia, C.; Zambelli, A. *Macromol. Rapid Commun.* **1996**, *17*, 333.